



Determination of Standard Free Energy of Formation for Niobium Silicides by EMF Measurements

Hiroyasu Fujiwara,^{a,z} Yukitomi Ueda,^a Alok Awasthi,^b Nagaiyar Krishnamurthy,^b and Sheo Parkash Garg^b

^aGraduate School of Energy Science, Kyoto University, Sakyo-ku, Kyoto 606-8501, Japan

^bBhabha Atomic Research Center, Materials Processing Division, Mumbai 400085, India

EMF measurements were carried out at temperatures ranging from 1280 to 1490 K in the following cells: $\ominus\text{Mo}, \text{Si} + \text{NbSi}_2 + \text{SiO}_2/\text{SiO}_2\text{-sat. Li}_2\text{O-SiO}_2/\text{NbSi}_2 + \text{Nb}_5\text{Si}_3 + \text{SiO}_2, \text{Mo} \oplus, \ominus\text{Mo}, \text{Si} + \text{NbSi}_2 + \text{SiO}_2/\text{SiO}_2\text{-sat. Li}_2\text{O-SiO}_2/\text{Nb}_5\text{Si}_3 + \text{NbO} + \text{SiO}_2, \text{Mo} \oplus$, and $\ominus\text{Mo}, \text{NbSi}_2 + \text{Nb}_5\text{Si}_3 + \text{SiO}_2/\text{SiO}_2\text{-sat. Li}_2\text{O-SiO}_2/\text{Nb}_5\text{Si}_3 + \text{NbO} + \text{SiO}_2, \text{Mo} \oplus$, using SiO_2 -saturated lithium silicate liquid electrolyte. Each of the cells showed a reliable electromotive force (emf) corresponding to the difference in silicon potential between the electrodes. Based on these emf values measured, the molar standard free energy of formation for NbSi_2 and Nb_5Si_3 were determined to be $\Delta G_{\text{NbSi}_2}^\circ/\text{kJ} = -165 + 0.008 (T/\text{K}) \pm 13$ and $\Delta G_{\text{Nb}_5\text{Si}_3}^\circ/\text{kJ} = -526 + 0.009 (T/\text{K}) \pm 63$, respectively.

© 2003 The Electrochemical Society. [DOI: 10.1149/1.1591757] All rights reserved.

Manuscript submitted October 15, 2002; revised manuscript received February 17, 2003. Available electronically July 1, 2003.

Pure niobium is commercially produced by a process involving aluminothermic reduction of niobium pentoxide. Another method proposed by the present authors^{1,2} is a silicothermic process involving reduction of niobium pentoxide and deoxidation of as-reduced niobium metal by silicon. In considering this process, thermodynamic data such as heat capacity, heat of formation, and free energy of formation for the compounds in the Nb-Si binary system became necessary. However, only limited information is available on these in the literature.³ Most of the reports⁴⁻¹⁴ for the heat of formation for NbSi_2 and Nb_5Si_3 are calculated and estimated values, except for the report by Gorelkin *et al.*¹⁰ and that by Meschel and Kleppa.¹¹ In these reports combustion calorimetry¹⁰ for Nb_5Si_3 and direct synthesis calorimetry¹¹ for NbSi_2 and Nb_5Si_3 were performed. Experimental evaluation of the heat capacity for NbSi_2 and Nb_5Si_3 are also limited.^{15,16} Further, no experimental work on the direct determination of the standard free energy of formation for niobium silicides has been reported.

In the present study, electromotive force (emf) measurements were carried out to determine the standard free energy of formation for NbSi_2 and Nb_5Si_3 . The temperature range investigated is 1280–1490 K. Based on the results, the standard heats of formation at 298 K for NbSi_2 and Nb_5Si_3 have also been obtained.

Thermodynamic Considerations

According to the binary Nb-Si phase diagram¹⁷ shown in Fig. 1, two niobium silicides, *i.e.*, Nb_5Si_3 and NbSi_2 , are stable at 1373 K. In the Nb-O binary system,¹⁷ three niobium oxides exist. Although the phase relation is clear for each of the binary systems in Fig. 1, the phase relation for the ternary Nb-Si-O system is not certain. In order to draw the isothermal section of the ternary phase diagram, a potential diagram, in which thermodynamically stable phases are related to the oxygen and silicon potentials, is constructed as in Fig. 2. The free energy of formation for each of the compounds that is necessary for this potential calculation has been obtained from Barin's table.⁴ Solid solubilities and the possibility of ternary compounds are ignored in this calculation.

In Fig. 2, three-phase equilibria is represented as a point and two-phase equilibria is represented as a line, except for the cases of SiO_2 and Si (these single-phase regions are shown as gray lines). The isothermal section for Nb-Si-O ternary at 1373 K shown in Fig. 1 is based on this potential diagram. Points A-F in Fig. 2 correspond to the three-phase triangles A-F, in Fig. 1. Locations of these points in Fig. 2 depend on the free energies of formation for the corresponding compounds. For example, the values of silicon activity,

a_{Si} , for points B and C are related to the standard free energy of formation for niobium silicides, $\Delta G_{\text{NbSi}_2}^\circ$ and $\Delta G_{\text{Nb}_5\text{Si}_3}^\circ$, respectively. In other words, if a_{Si} at point B and C is obtained, both $\Delta G_{\text{NbSi}_2}^\circ$ and $\Delta G_{\text{Nb}_5\text{Si}_3}^\circ$ can be determined. Considering that the main objective of the present work is the determination of $\Delta G_{\text{NbSi}_2}^\circ$ and $\Delta G_{\text{Nb}_5\text{Si}_3}^\circ$, measurements of emf corresponding to the difference in a_{Si} between points A and B, and between A and C in Fig. 2, are most suitable. However, because the experimental conditions are limited to the composition of SiO_2 saturation and metallic niobium and SiO_2 can never co-occur in Nb-Si-O ternary systems emfs corresponding to the difference in a_{Si} among points A, B, and D are measured in this study. The line CD corresponds to the following equilibrium



Thus

$$\log p_{\text{O}_2} = \frac{6}{5} \log a_{\text{Si}} + \frac{1}{5} \log K_{(1)} \quad [2]$$

where p_{O_2} and $K_{(1)}$ are the partial pressure of oxygen and the equilibrium constant for Reaction 1. The slope of this line is the fixed numerical value of 6/5, and the location of point D can be determined by the measurement of the difference in a_{Si} between points A and D. Then, a_{Si} at point C can be derived by using p_{O_2} at point C, which is the intersection of the line CD and the line corresponding to the p_{O_2} at the two-phase equilibria of Nb + NbO in Nb-O system.

In this way, a_{Si} at point B and C, *i.e.*, for $\Delta G_{\text{NbSi}_2}^\circ$ and $\Delta G_{\text{Nb}_5\text{Si}_3}^\circ$, can be obtained. It should be noted, however, that the standard free energy of formation of NbO, $\Delta G_{\text{NbO}}^\circ$, is necessary for determination of $\Delta G_{\text{NbSi}_2}^\circ$ and $\Delta G_{\text{Nb}_5\text{Si}_3}^\circ$ and that the accuracy of the literature data for $\Delta G_{\text{NbO}}^\circ$ influences the results of the present study.

Experimental

Assembled cells.—Three kinds of electrodes, in which the silicon potential is fixed by three-phase equilibria of Nb-Si-O ternary, were used for emf measurements, *i.e.*, electrode A: $\text{Si}(\text{s}) + \text{NbSi}_2(\text{s}) + \text{SiO}_2(\text{s})$; electrode B: $\text{NbSi}_2(\text{s}) + \text{Nb}_5\text{Si}_3(\text{s}) + \text{SiO}_2(\text{s})$; and electrode D: $\text{Nb}_5\text{Si}_3(\text{s}) + \text{NbO}(\text{s}) + \text{SiO}_2(\text{s})$. The letter representing each electrode corresponds to the characters used in Fig. 1 and 2. By choosing two electrodes from these three, three kinds of cells were constructed:

^z E-mail: fujiwara@energy.kyoto-u.ac.jp

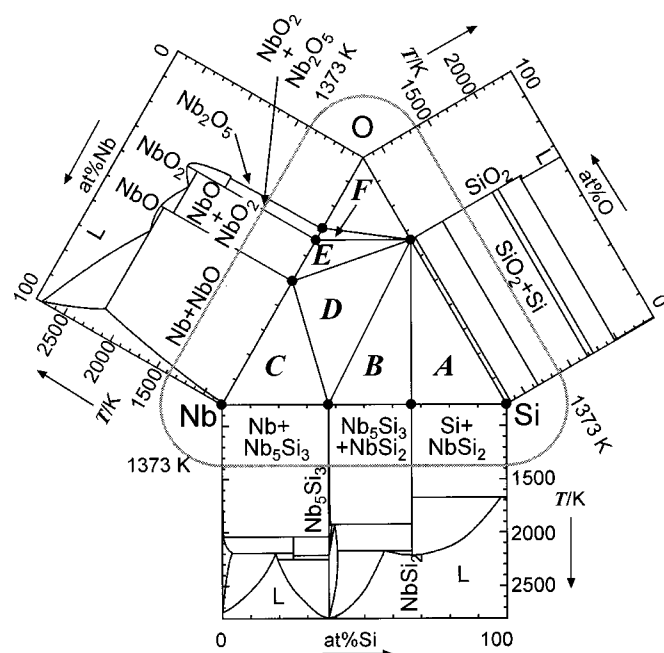


Figure 1. Phase diagrams of Nb-Si, Nb-O, and Si-O binary systems and isothermal section of Nb-Si-O ternary system at 1373 K.

cell AB: \ominus Mo, electrode-A/SiO₂-sat. Li₂O-SiO₂/
electrode-B, Mo \oplus [3]

cell AD: \ominus Mo, electrode-A/SiO₂-sat. Li₂O-SiO₂/
electrode-D, Mo \oplus [4]

cell BD: \ominus Mo, electrode-B/SiO₂-sat. Li₂O-SiO₂/
electrode-D, Mo \oplus [5]

Sakao and Elliott¹⁸ have reported measurement of silicon activity in Ag-Si alloys using lithium silicate electrolyte. In order to ensure the working of the present experimental setup, activity of Si in Ag-Si alloy using lithium silicate electrolyte was first measured, and the values obtained were compared with the values reported by them. The cell constructed for this purpose is:

cell(Ag): \ominus Mo, electrode-A/SiO₂-sat. Li₂O-SiO₂/
Ag-Si($x_{\text{Si}} = 0.054$), Mo \oplus [6]

Materials.—SiO₂ used was extra-pure grade from Wako Pure Chemical Industries, Ltd. NbSi₂ and Nb₅Si₃ were synthesized by vacuum heating of the mixture of pure elements. Appropriate amounts of niobium powder (99.9%, less than 74 μm , Furuuchi Chemical Co.) and silicon powder (99.999% less than 50 μm , Furuuchi Chemical) were mixed and pressed into 10 mm diam pellets. The pellets were placed on a molybdenum plate and heated inside a vacuum graphite furnace (10^{-2} to 10^{-3} Pa) at 1473 K for 7.2 ks. To complete the solid-solid reaction, they were continuously heated at 1873–1973 K for 7.2 ks. NbO was prepared by vacuum heating of the mixture of niobium powder and Nb₂O₅ (99.9%, Nakarai Chemical Co.). The heating operation was similar to that for silicides. Synthesized silicides and NbO were examined by X-ray diffraction (XRD) analysis.

The oxides and silicides thus prepared contained small amounts of some residual reactants, *i.e.*, NbO₂ in NbO, Nb₅Si₃ in NbSi₂, and Nb in Nb₅Si₃. This was apparently caused by evaporation of the high-vapor-pressure substances during the synthesis process. However, because of the preheating of the cell before the emf measure-

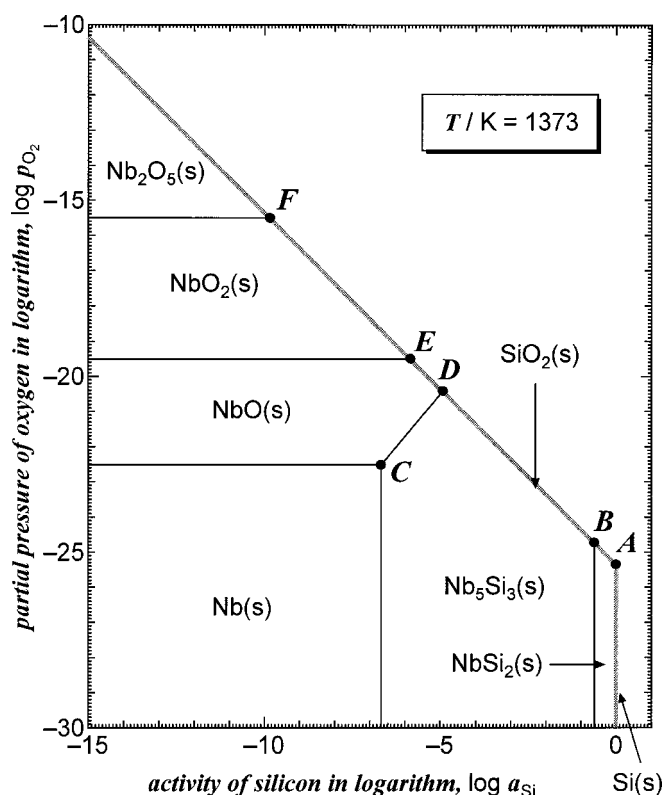


Figure 2. Potential diagram of Nb-Si-O ternary system at 1373 K. Points A-F correspond to the three-phase region shown in Fig. 1.

ment (*i.e.*, during “equilibration”), these residual reactants reacted and the electrode reached equilibrium. The electrodes were analyzed by XRD after the emf measurements, which confirmed disappearance of all these residual reactants. This disappearance suggests that these compounds do not participate in the three-phase equilibria of the electrodes.

Lithium silicate was prepared by heating in air the mixture of Li₂CO₃ and SiO₂ at 1173 K for 43.2 ks in a SiO₂ crucible. Dissociation of CO₂ from carbonate was ensured by weight change. The electrolyte composition was 86 mass % SiO₂. This composition corresponds to the SiO₂-liquidus at 1573 K in Li₂O-SiO₂ binary phase diagram.¹⁹ Ag-Si alloy used for cell(Ag), Eq. 6, was prepared by melting the pure metals in a graphite crucible under argon atmosphere.

Apparatus and procedure.—A schematic illustration of the experimental setup is shown in Fig. 3. A silicon carbide resistance furnace equipped with mullite reaction tube (g) of 52 mm i.d., 60 mm o.d., and 1000 mm length was used. Temperature was measured by a Pt + (Pt-13% Rh) thermocouple (i) placed inside a SiO₂ protection tube (h) and was controlled by PID type controller to ± 1 K. The cells were placed inside an outer SiO₂ crucible (c) of 36 mm o.d., 32 mm i.d., and 100 mm height, which in turn was placed in a graphite protection crucible (f).

At first, a molybdenum lead wire (j) of 0.5 mm diam and the pelletized electrodes (a), which was prepared by pressing the powder mixture of one set of the three compounds, were placed into an inner SiO₂ crucible (d) of 12 mm o.d., 10 mm i.d., and 10 mm height. A mullite insulating tube (e) was pushed into the gap between the inner SiO₂ crucible and the electrode pellet in order to avoid direct contact of molybdenum lead wire with the electrolyte. Four such inner SiO₂ crucibles (d) were used in every heating operation (Fig. 3, top view). Then these inner SiO₂ crucibles were put into the outer SiO₂ crucible (c) with powder SiO₂ and electrolyte

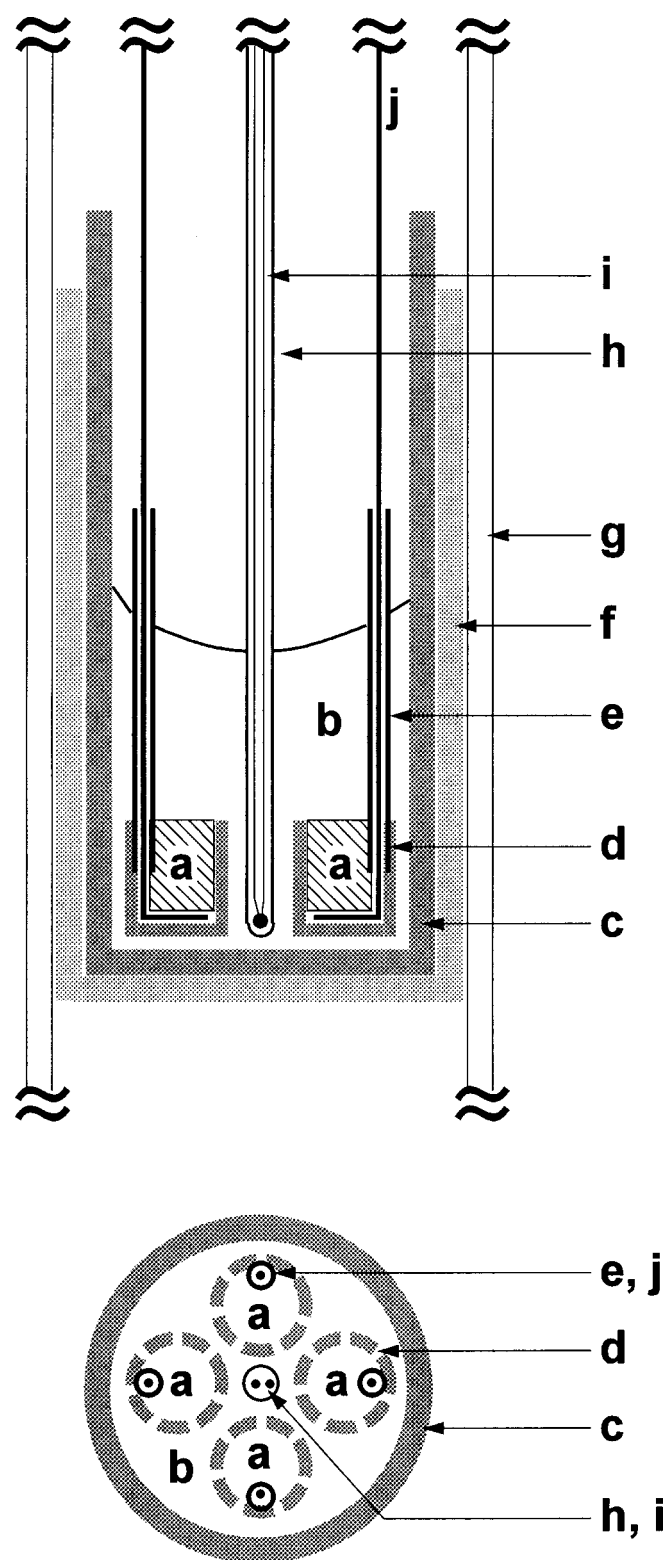


Figure 3. Schematic illustration of experimental apparatus: (a) electrode pellet, (b) SiO₂-saturated liquid electrolyte, (c) outer SiO₂ crucible, (d) inner SiO₂ crucible, (e) mullite insulating tube, (f) graphite protection crucible, (g) mullite reaction tube, (h) SiO₂ protection tube, (i) thermocouple, and (j) molybdenum lead wire.

(b). The upper part of each of the inner SiO₂ crucibles (d) was fully covered with electrolyte.

In order to establish the equilibrium between electrode and electrolyte, the cell was first heated to 1423–1473 K for 7.2–14.4 ks

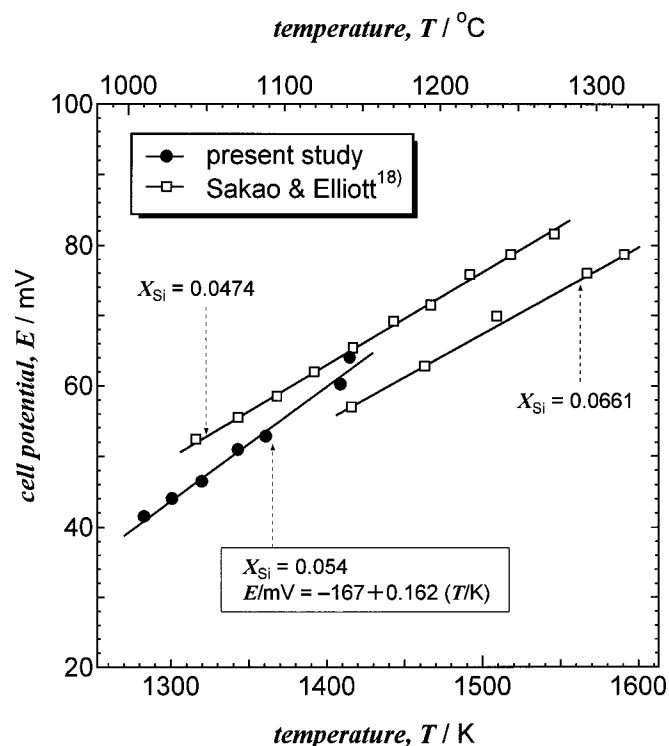


Figure 4. Observed emf of the cell $[\ominus \text{Mo}, \text{Si} + \text{NbSi}_2 + \text{SiO}_2 / \text{SiO}_2\text{-sat. Li}_2\text{O} + \text{SiO}_2 / \text{Ag} + \text{Si}(x_{\text{Si}} = 0.054), \text{Mo} \oplus]$ as a function of temperature and comparison with literature data.¹⁸

before starting the emf measurement. Each emf was obtained after holding at a constant temperature for more than 2.4 ks. Only emf values stable within 1 mV for 600 s were considered as equilibrium value. EMF was measured by digital voltmeter with 1 G Ω inner electric resistance. Reversibility of the electrochemical reaction was checked occasionally by passing a small amount of outer current through the cell for a moment. In this operation, emf was restored eventually. Stability of the emf was tested by holding the cell at a constant temperature for 43.2 ks. Measured emf values were reproducible within 1 mV.

Experimental procedure for cell(Ag) was almost the same as that for silicide electrodes, except for the location of the alloy electrode. To ensure good contact of the molten Ag-Si alloy with the electrolyte, the molten alloy was placed inside a SiO₂ tube (12 mm o.d., 10 mm i.d., and 60 mm length) with holes and kept on the electrolyte. The molybdenum lead wire was dipped into the molten alloy for measuring emf. After emf measurements, solidified Ag-Si alloy was dissolved in HF + HNO₃ solution and the silicon content was determined by inductively coupled plasma spectrometry.

Results and Discussion

Activity of silicon in Ag-Si alloy.—As electrode A contains pure silicon, the activity of silicon in this electrode is unity. Then the emf for this cell is given

$$E = -\frac{RT}{4F} \ln a_{\text{Si}} \text{ (in alloy)} \quad [7]$$

The emf values of the cell represented Eq. 7 are plotted against temperature in Fig. 4. In this figure, the results of Sakao and Elliott¹⁸ for alloys with nearby compositions ($x_{\text{Si}} = 0.0474$ and 0.0661) are also shown. The slope of the relation obtained by the present study is comparable to those reported by them, indicating that equilibrium was reached at various temperatures. Activity of silicon in the Ag-Si ($x_{\text{Si}} = 0.054$) alloy at temperatures (1323 and 1423 K) obtained

Table I. Activity of silicon in Ag-Si alloy ($x_{\text{Si}} = 0.054$).

Temperature, T/K	Present study	Sakao and Elliott ^a
1323	0.190	0.186
1423	0.126	0.130

^a Values read from graph.

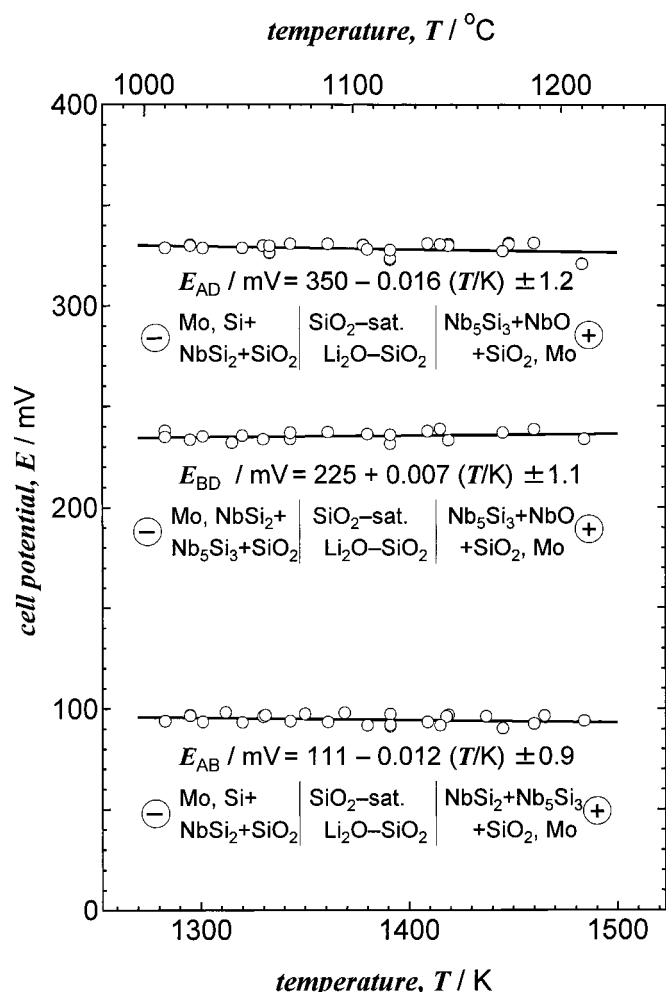
presently are listed in Table I along with those of Sakao and Elliott. The present results compare well with these values. The use of lithium silicate electrolyte in the present study was essentially the same as that by Sakao and Elliott. However, few points relating to the experiments were different, *e.g.*, the electrode without molten alloy and the electrolyte with a slightly different composition. These results apparently indicate that no problem was caused by these differences under the present experimental conditions.

EMF and activity of the three-phase equilibrium.—EMF of the cell AB, AD, and BD, E_{AB} , E_{AD} , and E_{BD} , are shown in Fig. 5. The emf-temperature relations obtained by the linear regression are

$$E_{\text{AB}}/\text{mV} = +111 - 0.012 (T/\text{K}) \pm 0.9 \quad [8]$$

$$E_{\text{AD}}/\text{mV} = +350 - 0.016 (T/\text{K}) \pm 1.2 \quad [9]$$

$$E_{\text{BD}}/\text{mV} = +225 + 0.007 (T/\text{K}) \pm 1.1 \quad [10]$$

**Figure 5.** Observed emf of cells AB, AD, and BD plotted against temperature.

respectively. It is clear that the temperature dependence of emf is relatively small for all three cells. This is so because only condensed phases are involved in the overall cell reactions, for which the entropy change is known to be small. Although emf measurements were carried out by increasing and decreasing temperature, no systematic difference was observed in the results. Each of the emf measurements of the cells were carried out independently. However, only two of them are arithmetically independent. Consistency in measurements can be seen by comparing measured emf-temperature relation (Eq. 10) with the following equation (Eq. 11)

$$E_{\text{BD}}/\text{mV} = +239 - 0.004 (T/\text{K}) \pm 1.5 \quad [11]$$

calculated using Eq. 8 and 9. The E_{BD}/mV values obtained at an average temperature of 1400 K from Eq. 10 and 11 are 234.8 ± 1.1 and 233.4 ± 1.5 , respectively.

Because a_{Si} at electrode A is unity, for cell AB and AD, the emf values, E_{AB} and E_{AD} , are given as

$$E_{\text{AB}} = -\frac{RT}{4F} \ln a_{\text{Si}}^{\text{B}} \quad [12]$$

$$E_{\text{AD}} = -\frac{RT}{4F} \ln a_{\text{Si}}^{\text{D}} \quad [13]$$

Then a_{Si} at the three-phase equilibrium at points B and D are obtained as functions of temperature within the experimental temperature range (1280–1490 K)

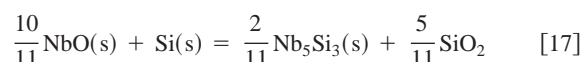
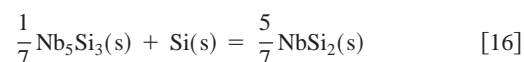
$$\log a_{\text{Si}}^{\text{B}} = +0.24 - 2240/(T/\text{K}) \pm 0.02 \quad [14]$$

$$\log a_{\text{Si}}^{\text{D}} = +0.32 - 7060/(T/\text{K}) \pm 0.02 \quad [15]$$

Using these equations, $\log a_{\text{Si}}$ values at points B and D at 1373 K are calculated to be -1.39 and -4.82 , respectively. The former value is about a 0.8 order of magnitude lower than that shown in Fig. 2.

Standard free energy of formation for silicides.—As mentioned previously, the only two emfs of the three cells AB, AD, and BD are arithmetically independent. Because the standard deviation of the linear regression is relatively low, emf of cells AB and BD are used for the calculation of the standard free energy of formation for silicides.

At electrodes B and D, the following equilibria are achieved, respectively



Thus, the activities of silicon at electrodes B and D are given as

$$RT \ln a_{\text{Si}}^{\text{B}} = +\frac{5}{7} \Delta G_{\text{NbSi}_2}^{\circ} - \frac{1}{7} \Delta G_{\text{Nb}_5\text{Si}_3}^{\circ} \quad [18]$$

$$RT \ln a_{\text{Si}}^{\text{D}} = +\frac{2}{11} \Delta G_{\text{Nb}_5\text{Si}_3}^{\circ} + \frac{5}{11} \Delta G_{\text{SiO}_2}^{\circ} - \frac{10}{11} \Delta G_{\text{NbO}}^{\circ} \quad [19]$$

where $\Delta G_{\text{SiO}_2}^{\circ}$ and $\Delta G_{\text{NbO}}^{\circ}$ are the standard free energy of formation for SiO_2 and NbO , respectively. The emf of cells AB and BD can be related to the standard formation free energy for silicides as

$$4FE_{\text{AB}} = -\frac{5}{7} \Delta G_{\text{NbSi}_2}^{\circ} + \frac{1}{7} \Delta G_{\text{Nb}_5\text{Si}_3}^{\circ} \quad [20]$$

$$4FE_{\text{BD}} = +\frac{5}{7} \Delta G_{\text{NbSi}_2}^{\circ} - \frac{25}{77} \Delta G_{\text{Nb}_5\text{Si}_3}^{\circ} - \frac{5}{11} \Delta G_{\text{SiO}_2}^{\circ} + \frac{10}{11} \Delta G_{\text{NbO}}^{\circ} \quad [21]$$

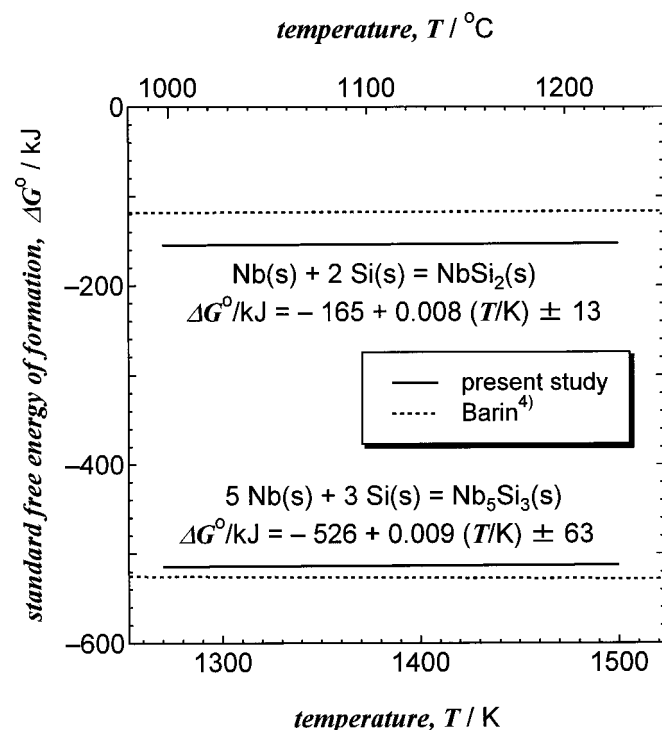


Figure 6. Comparison of standard free energies of formation for NbSi_2 and Nb_5Si_3 obtained with the literature data.

By solving these equations and using literature data²⁰ for $\Delta G_{\text{SiO}_2}^\circ$ and $\Delta G_{\text{NbO}}^\circ$, $\Delta G_{\text{NbSi}_2}^\circ$ and $\Delta G_{\text{Nb}_5\text{Si}_3}^\circ$ are obtained as functions of temperature

$$\Delta G_{\text{NbSi}_2}^\circ/\text{kJ} = -165 + 0.008 (T/\text{K}) \pm 13 \quad [22]$$

$$\Delta G_{\text{Nb}_5\text{Si}_3}^\circ/\text{kJ} = -526 + 0.009 (T/\text{K}) \pm 63 \quad [23]$$

The experimental errors in emf measurements of cells AB and BD are 0.9 and 1.1 mV, respectively. These errors result in 1 and 3 kJ mol^{-1} in accuracy of $\Delta G_{\text{NbSi}_2}^\circ$ and $\Delta G_{\text{Nb}_5\text{Si}_3}^\circ$. Inaccuracies of $\Delta G_{\text{SiO}_2}^\circ$ and $\Delta G_{\text{NbO}}^\circ$ are estimated from the standard heat of formation of SiO_2 and NbO , and are ± 1.7 and $\pm 12.6 \text{ kJ mol}^{-1}$,²⁰ respectively. Therefore, the overall inaccuracies for $\Delta G_{\text{NbSi}_2}^\circ$ and $\Delta G_{\text{Nb}_5\text{Si}_3}^\circ$

are calculated to be ± 13 and $\pm 63 \text{ kJ mol}^{-1}$, respectively. The experimental error in temperature measurements is ignored because of its relatively minor effect. Considering that 5 mol of niobium is consumed in the formation reaction of 1 mol Nb_5Si_3 , the fact that the calculated inaccuracy of $\Delta G_{\text{Nb}_5\text{Si}_3}^\circ$ is five times as large as that of $\Delta G_{\text{NbSi}_2}^\circ$ indicates the very large uncertainty that could be introduced by uncertainty of the value of $\Delta G_{\text{NbO}}^\circ$. As far as the present experimental method is applied, the electrode composition is limited to SiO_2 saturation. In other words, emf measurements corresponding to the difference in Si potential between point C and point A or B in Fig. 2 cannot be performed, as pointed out previously. Thus, the relatively high level of inaccuracy cannot be avoided.

Figure 6 shows the standard free energy of formation of niobium silicides. As shown in this figure, temperature dependence of the standard free energies is negligibly small. The present results for Nb_5Si_3 agree with the literature data⁴ and the temperature dependence of the free energy for both silicides is coincident. The present result for NbSi_2 is about 40 kJ lower than the literature data in the experimental temperature range. Even if the accuracy of the present data is considered, this difference is apparent.

The standard heats of formation of silicides.—By applying the third law method, the standard heat of formation of silicides at 298 K, $\Delta H_i^\circ(298)$, is given as

$$\Delta H_i^\circ(298) = \Delta G_i^\circ(T) - \Delta f_{\text{ef}} \cdot T \quad [24]$$

where Δf_{ef} is the change in the free energy function for the formation reactions of the silicides.⁴ The calculated values are listed in Table II. As the difference in $\Delta H_{(\text{NbSi}_2)_{1/3}}^\circ(298)$ and $\Delta H_{(\text{Nb}_5\text{Si}_3)_{1/8}}^\circ(298)$ calculated by using the free energy values of 1300 and 1400 K was less than 0.3 kJ, the averages of them are adopted in the Table. The estimated error in this Table was calculated from Eq. 22 and 23.

As mentioned before, the experimental data for $\Delta H_i^\circ(298)$ were reported by Gorelkin *et al.*¹⁰ ($i = \text{Nb}_5\text{Si}_3$) and Meschel and Kleppa¹¹ ($i = \text{NbSi}_2$ and Nb_5Si_3). The present results for NbSi_2 and Nb_5Si_3 agree with these literature data within the error limits, respectively. Based on the assessed data by Chart,⁶ Kubaschewski *et al.*,⁵ and Barin⁴ and on the experimental data by Meschel and Kleppa,¹¹ $\Delta H_i^\circ(298)$ for Nb_5Si_3 is more negative than that for NbSi_2 . This tendency is in accord with the present results.

Table II. Comparison of values of standard heats of formation of niobium silicides reported by various workers.

Source	Reference	Method	$\Delta_f H_i^\circ(298)/\text{kJ mol}^{-1}$	
			$(\text{NbSi}_2)_{1/3}$	$(\text{Nb}_5\text{Si}_3)_{1/8}$
Present study		EMF measurement	-53.9 ± 4.2	-62.2 ± 7.9
Barin	4	Assessment	-41.8	-63.8
Kubaschewskii <i>et al.</i>	5	Assessment	-46.0 ± 13.9	-56.5 ± 13.6
Chart	6	Assessment	-46.0	-60.7
Niessen and Boer	7	Calculation	-46	
Kaufmann	8	Calculation	-90.7	-65.3
Fernandes <i>et al.</i> ^a	9	Calculation	-55.5	-62.7
Fernandes <i>et al.</i> ^a	9	Calculation	-56.0	-60.9
Gorelkin <i>et al.</i>	10	Calorimetry		-63.8 ± 11.5
Mischel and Kleppa	11	Calorimetry	-53.7 ± 1.6	-64.6 ± 2.4
Schafer	12	Estimation		≤ -13.3
Searcy	13	Estimation	-42 ± 20	-33 ± 16
Brewer and Krikorian	14	Estimation	-24 to -78	-13 to -98

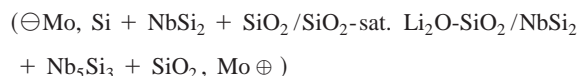
^a Two different models are applied.

Conclusions

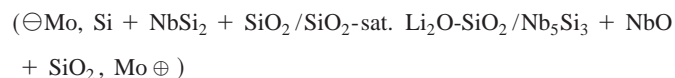
In order to determine the standard free energy of formation of niobium silicides, emf measurements were conducted at temperatures ranging from 1280 to 1490 K. The results are as follows:

1. The emf-temperature relations are

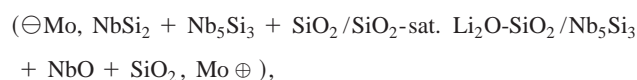
$$E/\text{mV} = +111 - 0.012 (T/\text{K}) \pm 0.9$$



$$E/\text{mV} = +350 - 0.016(T/\text{K}) \pm 1.2$$



$$E/\text{mV} = +225 + 0.007 (T/\text{K}) \pm 1.1$$



respectively.

2. Activity of silicon for three-phase equilibria of $\text{NbSi}_2 + \text{Nb}_5\text{Si}_3 + \text{SiO}_2$ and $\text{Nb}_5\text{Si}_3 + \text{NbO} + \text{SiO}_2$ are

$$\log a_{\text{Si}} = +0.24 - 2240/(T/\text{K}) \pm 0.02$$

$$(\text{for } \text{NbSi}_2 + \text{Nb}_5\text{Si}_3 + \text{SiO}_2)$$

$$\log a_{\text{Si}} = +0.32 - 7060/(T/\text{K}) \pm 0.02$$

$$(\text{for } \text{Nb}_5\text{Si}_3 + \text{NbO} + \text{SiO}_2)$$

respectively.

3. The standard free energy of formation for niobium silicides are

$$\Delta G_{\text{NbSi}_2}^0/\text{kJ} = -165 + 0.008 (T/\text{K}) \pm 13$$

$$\Delta G_{\text{Nb}_5\text{Si}_3}^0/\text{kJ} = -526 + 0.009 (T/\text{K}) \pm 63$$

4. The standard heats of formation for niobium silicides at 298 K are

$$\Delta H_{(\text{NbSi}_2)_{1/3}}^0(298)/\text{kJ} = -53.9 \pm 4.2$$

$$\Delta H_{(\text{Nb}_5\text{Si}_3)_{1/8}}^0(298)/\text{kJ} = -62.2 \pm 7.9$$

Acknowledgment

Honest experimental works done by Mr. Ishiwari (former undergraduate student of Kyoto University) and helpful comments and suggestions by Dr. Asano (Professor Emeritus, Kyoto University) and Dr. Wakasugi (Kyoto Institute of Technology) are gratefully acknowledged. This study was financially supported by a Grant in Aid of the Japanese Ministry of Education, Culture, Sports and Technology (no. 14550722).

Kyoto University assisted in meeting the publication costs of this article.

References

1. A. Awasthi, N. Krishnamurthy, Y. J. Bhatt, R. Venkataramani, Y. Ueda, and S. P. Garg, *J. Alloys Compd.*, **265**, 190 (1998).
2. A. Awasthi, Y. J. Bhatt, N. Krishnamurthy, Y. Ueda, and S. P. Garg, *J. Alloys Compd.*, **315**, 187 (2001).
3. M. E. Shlesinger, H. Okamoto, A. B. Gokhale, and R. Abbaschian, *J. Phase Equilib.*, **14**, 502 (1993).
4. I. Barin, *Thermodynamic Data of Pure Substances*, 3rd ed., VCH Verlagsgesellschaft mbH, Weinheim (1995).
5. O. Kubaschewski, C. B. Alcock, and P. J. Spencer, *Materials Thermochemistry*, 6th ed., Pergamon Press, Oxford (1993).
6. T. G. Chart, *High Temp.-High Press.*, **5**, 241 (1973).
7. A. K. Niessen and F. R. De Boer, *J. Less-Common Met.*, **82**, 75 (1981).
8. L. Kaufman, *CALPHAD: Comput. Coupling Phase Diagrams Thermochem.*, **3**, 45 (1979).
9. P. B. Fernandes, G. C. Coelho, F. Ferreira, C. A. Nunes, and B. Sundman, *Intermetallics*, **10**, 993 (2002).
10. O. S. Gorelkin, A. S. Dubrovin, O. D. Kolesnikova, and N. A. Chirkov, *Russ. J. Phys. Chem.*, **46**, 431 (1972).
11. S. V. Meschel and O. J. Kleppa, *J. Alloys Compd.*, **274**, 193 (1998).
12. Von H. Schafer and K. D. Dohmann, *Z. Anorg. Chem.*, **299**, 197 (1959).
13. A. W. Searcy, *J. Am. Ceram. Soc.*, **40**, 431 (1957).
14. L. Brewer and O. Krikorian, *J. Electrochem. Soc.*, **103**, 38 (1956).
15. V. P. Bondarenko, V. I. Zmii, E. N. Formichev, A. A. Kalashnik, and N. P. Slyusar', *High Temp.*, **8**, 856 (1970).
16. V. P. Bondarenko, L. A. Dvorina, N. P. Slyusar', and E. N. Formichev, *Sov. Powder Metall. Met. Ceram.*, **10**, 892 (1971).
17. T. B. Massalski, H. Okamoto, P. R. Subramanian, and L. Kacprzak, *Binary Alloy Phase Diagrams*, 2nd ed., ASM International, Materials Park, OH (1990).
18. H. Sakao and J. F. Elliott, *Metall. Trans. B*, **5B**, 2063 (1974).
19. E. M. Levim, C. R. Robbins, and F. McMurdie, *Phase Diagrams for Ceramists*, Vol. 1, The American Ceramic Society, Ohio (1964).
20. N. W. Chase, Jr., C. A. Davis, J. R. Downey, Jr., D. J. Frurip, R. A. McDonald, and A. N. Syverud, *JANAF Thermochemical Tables*, 3rd ed., American Chemical Society and American Institute of Physics, New York (1985).